Mussels repair shell damage despite limitations imposed by ocean acidification

Matthew N. George*[1,2], Michael J. O'Donnell[1,2,3], Michael Concodello[4], and Emily Carrington[1,2]

1 – Friday Harbor Laboratories, University of Washington, Friday Harbor, WA, 98250, USA

2 – Department of Biology, University of Washington, Seattle, WA, 98195, USA

3 – Current Address: Department of Bioengineering, University of California, Berkeley, Berkeley, CA 94720

4 – Department of Biology, University of Rhode Island, Kingston, RI, 02881, USA

*Corresponding author: mngeorge@uw.edu

keywords: boring predation, biomineralization, calcification, *Mytilus edulis*, *Mytilus trossulus*

Abstract

Bivalves frequently withstand shell boring attempts by predatory gastropods that result in shell damage that must be quickly repaired to ensure survival. While the processes that underlie larval shell development have been extensively studied within the context of ocean acidification (OA), it remains unclear whether shell repair is impaired by elevated pCO_2. To better understand the stereotypical shell repair process, we monitored mussels (*Mytilus edulis*) with sublethal shell damage within both field and laboratory conditions to characterize the deposition rate, mineral composition, and structural integrity of repaired shell. These results were then compared with a laboratory experiment wherein mussels (*Mytilus trossulus*) repaired shell damage in one of seven pCO_2 treatments (400–2500 µatm). Shell repair proceeded through four distinct stages; shell damage was first covered with an organic film, then mineralized over the course of weeks, acquiring the appearance of nacre after 8 weeks. OA did not impact the ability of mussels to close drill holes, nor the strength or density of the repaired shell after 10-weeks, as measured through mechanical testing and µCT analysis. However, as mussels progressed through each repair stage, significant interactions between pCO_2, the length of exposure to treatment conditions, and the strength, inorganic content, and physiological condition of mussels within OA treatments were observed. These results suggest that, while OA may not prevent mussels from repairing shell damage, sustained exposure to elevated pCO_2 may induce physiological stress responses that impose energetic constraints on the shell repair process.

1. Introduction

Mytilid mussels are bivalve mollusks that perform ecologically important roles within marine ecosystems [1,2] and support an intercontinental fishery that accounts for 6.9% (1.2 million tonnes) of the 250 billion USD global aquaculture industry [3]. Mussels survive harsh conditions along coastal shores using bivalve shells that protect them from waves, predators, and desiccation [4]. Nearshore ecosystems are subject to substantial environmental variability, including fluctuations in seawater pH [5]. As a consequence of abiotic and biotic nearshore processes, mussels routinely endure exposure to acidified conditions (with respect to open ocean conditions), resulting in pH reductions of up to 1 unit for hours or days at a time [6-8]. Ocean acidification (OA), or the incremental decline in oceanic pH globally that results from the uptake of anthropogenic atmospheric pCO_2 by the ocean [9,10], is expected to intensify this process, resulting in significant consequences for marine shelled organisms [11]. Given their ecological and economic importance, the ability of mussels to build, maintain, and repair damaged shell under different pCO_2 conditions will determine the impact that OA has on ecological communities and aquaculture production [12,13].

In the rocky intertidal, the distribution of mussels along shorelines is limited by wave forces [14] and motile predators (e.g., sea stars, crustaceans) that pry or peel open the shells of bivalves [15,16]. Other shallow water predators include marine snail species (muricid and natricid gastropods) that “drill” through the shell to access their prey [17,18]. Gastropod predation is characterized by alternating bouts of mechanical shell damage and enzymatic digestion, where damage is induced using a toothed radula (bouts of 1-2 minutes) followed by the secretion of specialized enzymes (bouts of 25-30 minutes) [19,20]. Using this method, whelks can bore into and fully digest a mussel within a few days. The removal of mussels from bed networks by shell boring organisms contributes to mussel dislodgement and can cause cascading effects on intertidal ecosystems [21,22].

Due in part to the relatively long handling time of their feeding strategy and the dynamic environment of the intertidal zone, shell boring gastropods are not always successful [23]. Evidence of incomplete and repaired boreholes can be seen throughout the fossil record, indicating that mollusks survive encounters with gastropod predators and persist with shell damage [24]. However, shell damage can impose a cost; in surveys where mussel populations were inundated with phototrophic endoliths, sublethal shell damage accompanied an increase in adult mortality of up to 50% [25]. Holes in a mussel's shell can increase desiccation risk during low tide, expose the extracellular mantle cavity to microbial infection, promote the invasion of predatory amphipods and/or mobile polycheates, and hinder internal acid-base regulation [26].

Mussel shell is composed of three distinct layers. The inner layer (nacre, 'mother-of-pearl') is made up of tabloid aragonite crystals, while the middle layer is an aggregate of calcium carbonate arranged in calcite prisms, and the outer layer is a proteinaceous covering known as the periostracum [27,28]. The mantle tissue that produces shell is composed of three zones, with the outer mantle (marginal and pallial zones) producing both calcite and aragonite during shell growth, while the inner mantle (central zone) produces aragonite and is involved in shell thickening and repair [29]. Shell formation typically proceeds in two phases, wherein the mantle extrudes a mixture of polysaccharides and glycoproteins that form an organic matrix that facilitates the formation of calcium carbonate crystals [30]. Previous work suggests that the creation and maintenance of shell is particularly costly, in large part due to the formation of this proteinaceous scaffolding [31,32]. OA has been proposed to impact shell formation through both direct and indirect mechanisms, including a decrease in carbonate ion (CO^{2-}_3) availability with declining pH [33,34], and pH-induced metabolic stress that disrupts the intercellular transport mechanisms that support the production of calcium carbonate [35].

The effect of OA on shell formation at the growth margin in mussels has been well studied [11,36-38], particularly in the context of larval development [39,40], and in the presence of warming [41-43]. Aragonite saturation-state has been shown to be the most influential variable in juvenile mussel and oyster calcification [34]. While not extensively studied in adults, OA can impose metabolic constraints on the biomineralization process [44], resulting in changes in shell shape and thickness [45]. These results suggest that declines in oceanic pH could impact how mussels recover from incomplete predation events such as those imposed by marine gastropods. However, uncertainty still exists as to the extent to which the processes that underlie shell repair mimics biomineralization at the shell margin [46], and whether the repair process in adults is subject to the same kinetic constraints as in early shell development [47].

Here we present data collected from observations and experiments conducted in the rocky intertidal of Rhode Island, USA on the blue mussel (*Mytilus edulis*; Linnaeus, 1758) and an OA laboratory experiment conducted in Washington, USA on the pacific blue mussel (*Mytilus trossulus*; Gould, 1850). Our field observations and experiments serve to determine the frequency with which mussels survive shell boring events and provide a timeline of the shell repair process that mussels undergo after incurring sublethal shell damage. These results were then used to inform laboratory mesocosm experiments wherein mussels repaired shell damage that mimicked the damage imposed by shell boring gastropods under seven OA treatments (pCO_2 targets: 400–2500 µatm) for up to 10 weeks. The impact of environmental pCO_2 on the progression of the shell repair process, as well as the mineralization and strength of repaired shell were then assessed through material composition analysis, mechanical testing, and µCT analysis.

2. Materials and Methods

Datasets presented here are the compilation of field and laboratory experiments undertaken on the Atlantic and Pacific coasts of the United States, utilizing two species of *Mytilid*

mussels, *Mytilus edulis* and *Mytilus trossulus*, respectively. Initial field observations of the frequency of shell repair in *M. edulis* populations was collected over three years (1998–2000) during monthly mussel bed surveys within the intertidal near Bass Rock and Black Point in Rhode Island, USA, (41°24' 17.4"N, 71°27' 30.5"W and 41°23' 42.4"N, 71°27' 47.9"W), following previously described sampling methods [48,49]. The observation that mussels frequently sustained and repaired shell damage from boring predators (Figure 1) motivated field experiments during the summer of 2003 wherein shell damage was induced in *M. edulis* living within bed populations at Black Point and resampled over the course of two months to investigate the repair process (Figure 2, Figure 3). Results of these field experiments were subsequently used to inform a laboratory experiment investigating the effect of ocean acidification (OA; elevated seawater pCO_2, decreased pH) on the shell repair process in *M. trossulus*, conducted during the summer of 2012 at Friday Harbor Laboratories, located on San Juan Island, Washington, USA (48°32' 46.9"N, 123°00' 36.5"W).

M. trossulus and *M. edulis* are closely related sister taxa that naturally occur in sympatric populations along the eastern and western coasts of the United States. Due to their genetic similarity and systematic inclusion, along with the mediterranean mussel (M. galloprovincialis), within the 'Mytilus edulis complex' [50,51], hybridization between the two species is common [52,53]. While members of the complex have similar growth rates and physiology [54], shell characteristics can vary. For example, *M. edulis* typically produces stronger, thicker shells than *M. trossulus*, with the magnitude of this species difference varying by site [55]. However, the material properties and composition of shell (e.g., Young's modulus, Vicker's hardness, calcite/aragonite crystallographic orientation, etc.) within *M. edulis* and *M. trossulus* are not significantly different [56], suggesting their response to shell damage within this study is comparable.

Throughout field and laboratory experiments several measurement techniques remained consistent. Whenever a mussel was sampled, shell length of the major valve axis was measured with vernier calipers (Wiha-41102, ± 0.01 cm). Mussel condition and reproductive status was also commonly assessed by resecting and separating gonad and somatic tissue and drying each at 60°C until a stable weight was achieved. Condition index (CI) was defined as the ratio of total dry tissue mass to shell length cubed [57], while gonad index (GI) was defined as the ratio of the dry gonad mass to dry somatic tissue mass (Metler Toledo ML54, ± 0.01 g) as previously described [48].

To assess the progression of shell repair through distinct repair stages, shells were dried at room temperature, photographed with a length standard, and qualitatively scored from 0 to 4. Shells that had no visible evidence of repair were assigned to stage 0 (S0). Shells where organic matrix covered drill holes (or was present elsewhere) were considered to be at stage 1 (S1). Stage 2 (S2) was characterized by a mixture of organic and mineral material, while stage 3 (S3) was assigned when repaired shell was completely mineralized and rough in texture. Repaired shell at stage 4 (S4) were considered to be visually indistinct from the surrounding shell material and resembled the surface characteristics and color of nacre. Examples of each stage are outlined in Figure 2A.

The size of shell repair patches at each stage were quantified by photographing the shell interior and tracing the outline of the repaired region to determine the cross-sectional area (±0.01 cm^2) using Image J. [58]. The strength of the repaired shell was assessed using an Instron 5565 material testing frame [59] fitted with a micro-indentation steel tip (diameter = 0.5 mm). Repaired shell was approached from the exterior of the shell at 10 mm min^{-1} and the resulting maximum force required to dislodge the repaired region from drill holes was recorded (±0.01 N). This assay was not designed to be a comprehensive analysis of the material properties of repaired shell, but

rather to approximate the effort a predator would have to exert to re-enter the mantle cavity and serve as an estimation of the ability of the repair to prevent subsequent predation. Finally, the inorganic content (%) of the repaired shell was determined by removing newly deposited material from shell injuries and comparing their mass before and after incineration at 500°C for 4 hours [60].

2.1. Rhode Island: field experiment

The ability of *M. edulis* (shell length = 3-5 cm) to repair simulated shell damage that approximated the size and shape of shell injuries imposed by boring gastropods was first assessed within intertidal mussel beds located near Black Point, Rhode Island, USA. A 1 mm diameter hole was carefully drilled in the apex of the right valve of mussels *in situ* without removing mussels from aggregations, using a drill stop of 1 mm to prevent injury to the internal tissues of the animal. Mussels chosen for inclusion in the experiment were at similar tidal heights (ranging from 0.5 m above and below MLLW) and within three meters of each other to ensure consistent wave exposure and environmental conditions. After shell damage, mussels were sampled over the course of two months (June–July, 2003) approximately biweekly (10, 23, 38, and 51 days). Upon collection, animals were sacrificed and the CI and GI of each was determined; these metrics were compared with an initial sample of nearby mussels taken on the day shell damage was initiated. Shells were visually assessed for shell repair (qualitative score S0-S4), and the cross-sectional area of the repaired region (cm^2), the force required to dislodge the shell repair (N), and the inorganic content (%) of newly produced shell were measured as previously described.

2.2. Washington State: laboratory ocean acidification experiment

M. trossulus (shell length = 3-5 cm) were collected from Argyle Creek, San Juan Island, WA, USA (48-31'12'' N, 123-00'53'' W) in March, 2012. Upon collection, a subset of mussels was immediately sampled for initial field values of GI and CI. Shell damage was induced in the right

valve of remaining mussels as previously described and individuals were haphazardly placed in one of seven experimental mesocosms that ranged in target pCO_2 levels (400, 700, 1000, 1600, 1900, 2200, 2500 µatm) at 16°C in the Ocean Acidification Environmental Laboratory (OAEL) located at Friday Harbor Laboratories, San Juan Island, WA, USA. Mussels were held in 1.5L chambers with flow-through, UV-sterilized, and 0.2 µm filtered seawater. Chambers were cleaned three times weekly. Mussels were fed a diet of prepared algal paste (Shellfish Diet 1800, Reed Mariculture, Campbell, CA) at a daily rate of 5% of the estimated biomass within each chamber. Mussels were removed from each treatment over the course of a 2.5-month exposure at irregular intervals (8, 15, 22, 28, 43, 56, 69 days) and the GI, CI, cross-sectional area of the repaired shell region, as well as the strength and inorganic content of repaired shell were determined as previously described.

OA treatments were accomplished through dynamic injection of CO_2 using a pH-stat system, following the methods outlined in O'Donnell et al. 2013 [61]. Briefly, a Honeywell UDA2182 process controller and Honeywell Durafet III electrode [62] monitored the pH (uncertainty = ± 0.13%) and temperature (uncertainty = ± 0.63%) of each experimental mesocosm and added CO_2 to maintain the pH at a predefined setpoint calculated from target pCO_2 levels using CO2calc [63]. pH electrodes were calibrated to the total scale using spectrophotometric pH (Ocean Optics USB4000; Ocean Insight, Toms River, NJ) and were compared to treatment conditions every 3-4 days to ensure the correct calibration was maintained. The salinity of each treatment was measured daily using a sensION 5 conductivity meter (Hach Company, Loveland, CO; uncertainty = ± 0.33%). Total alkalinity (A_T) was measured using SOP 3b from (Dickson *et al.*, 2007) every 3-4 days (uncertainty = ± 0.33%).

The relationship between A_T and salinity established over the course of two years at our field station (A_T = 38.856 * Salinity + 916.43, R^2 = 0.95) was used to estimate A_T in each

mesocosm; results obtained by this method were found to be within ± 0.4% of measured A_T values. From estimates of A_T and measurements of pH, temperature, and salinity, we calculated the pCO_2 (µatm), CO_3 (µmol kg^{-1} SW), HCO_3 (µmol kg^{-1} SW), aragonite saturation state (Ω_{ar}), and calcite saturation state (Ω_{ca}) of each treatment. The uncertainty associated with each calculated parameter was determined using a Monte Carlo analysis (i = 10,000), sampling the random, normal distribution of measurement uncertainty associated with each pH, A_T, temperature, and salinity measurement and propagating them through each calculation. The resulting propagated uncertainty was combined with treatment variability (1 S.D.) by taking the square root of the sum of squares (reported as total uncertainty (u_T)), following published recommendations [64].

Microtomography (microCT) scans of shells from mussels in OA treatments were taken using a Skyscan 1076 scanner (Bruker, Billerica, MA), imaging shells in 35 µm slices at 45 kV. 3D image reconstruction was performed in NRecon (Micro Photonics Inc, Allentown, PA), with further rendering in Drishti [65]. The density of repaired shell was estimated by applying a 1 mm diameter cylinder centered on the drill hole of each shell and recording the mean and maximum grayscale values of the scan slices in aggregate. Grayscale values were compared with those of unrepaired shell 1 mm away from the drill hole.

2.3. Statistical Analyses

All statistical analyses were performed in R (Version 3.4.1; http://www.r-project.org/) using the RStudio IDE (Version 1.0.153; http://www.rstudio.com/). When applicable, analysis of covariance (ANCOVA) was used to investigate differences in response variables to the duration of exposure (days) and magnitude (pCO_2 targets) of OA treatments. During model construction, the assumptions of normality and homoscedasticity were assessed using the Shapiro test and a visual assessment of Q-Q and residual-fitted plots. To achieve normality, the Johnson transformation was used when necessary [66]. When response variables were expressed as

proportions, the logit transformation (log of odds ratio) was used. For significant effects ($\alpha = 0.05$), the agricolae package was used to perform pairwise comparisons of groups using the Tukey HSD post hoc test [67]. For the comparison of qualitative repair scores, the distribution of mussels within each stage was compared with a chi-squared test, using the 400 µatm treatment as the expected values.

3. Results

3.1. Rhode Island: field experiment

Evidence of gastropod predation within mussel beds varied significantly during monthly field sampling of intertidal sites, with as many as 8% of mussels (*M. edulis*, n=50, 1998-2001) within bed populations carrying shell damage in a given month (Figure 1B). When shell damage was artificially induced in a subset of individuals within a population, mussels progressed steadily through each repair stage (S0-S4) over a 51-day period (see Figure 2A for examples). Ten days after shell damage was induced, 70% of mussels had entered the first stage of shell repair (S1) and successfully closed drill holes by applying an organic film over the opening (examples from *M. trossulus* provided in Figure 3). These results matched laboratory assays wherein it took *M. trossulus* (n=25) 11 days for all mussels to reach S1 (Figure 2B). Following the closure of the shell opening, 86.6% of mussels were at S2 after 23 days, and 80% were at S3 after 38 days (Figure 2C).

Significant changes in the material and biomechanical properties of repaired shell were observed as mussels progressed through each repair stage. The inorganic content ($p<0.001$, Figure 2D) and force required to dislodge repaired shell material ($p<0.001$, Figure 2E) significantly increased as mussels (*M. edulis*) remained within the intertidal post shell injury by +83% and +346% (comparing 10 to 51 days), respectively. For both measured parameters, hardening of the repaired region corresponded with the transition from S1 to S2 (Figure 2C-E). The relationship

between repair stage and the physical properties of repaired shell was further validated by pooling data from field experiments (*M. edulis*) and laboratory studies discussed in the following section (*M. trossulus*). From this analysis, repair stage was positively correlated with inorganic content ($p=0.012$; Figure 2F) and force ($p=0.032$; Figure 2G). The strength of repaired shell and inorganic content were also positively correlated (loess regression) with each other when compared across both species, with inorganic content explaining 42% of the variance observed in force ($p<0.001$, Figure 2H).

At the end of the field experiment, the appearance of repaired shell resembled that of surrounding shell, with all mussels proceeding to at least S3 after 51 days; in this end stage population, 45% of repairs were in S4 and had evidence of nacre formation (Figure 2C). However, when mechanical testing was employed to dislodge the repaired region of shell repairs within S4, the force required was not significantly different than those in S2 or S3 (Figure 2G), indicating that perhaps more time is needed to produce a material with a similar structural integrity to undamaged shell. µCT imaging of shells at S3 and S4 suggested that repaired shell had a similar density to unrepaired shell, but appeared thinner in cross-section and was irregularly anchored to the interior shell around each drill hole (Figure 4C,D).

3.2. Washington State: ocean acidification shell repair experiment

Laboratory experiments employed seven OA treatments, with measured pH values ranging from 7.29 to 7.95 (total scale, Table 1) and calculated pCO_2 levels ranging from 483 to 2458 µatm (Table 2). OA did not significantly affect whether mussels were able to repair damaged shell ($p=0.53$, Table S1), with no observed impact of pCO_2 on the proportion of mussels that mineralized repaired shell (reached S3 or S4) after 4 weeks (Figure 5A). All mussels closed drill holes irrespective of treatment, with no impact of pCO_2 ($p=0.64$) or time ($p=0.57$) on the size of the S1 repair patch (Table S3). Repair patches were generally proportional to the degree of shell

damage, neatly covering the drill hole in 60% of cases (Figure 3F). However, significant overgrowth of the repair patch did occur, resulting in organic matrix deposition within the entire valve interior (Figure 3D) and repair away from the shell defect in rare cases (Figure 3E).

While OA did not prevent mussels from closing shell injuries or mineralizing repaired shell, the severity pCO_2 exposure and the time spent within treatments significantly impacted the inorganic content (OA: $p<0.001$, time: $p<0.001$; Table S3, Figure 5B) and the force required to dislodge repaired regions (OA: $p<0.001$, time: $p=0.02$; Table S3, Figure 5C). Similar results were observed when analyses were constrained to only include mussels after 10 weeks within treatments (end point only). After 10-weeks of OA exposure, significantly fewer animals reached S3 or S4 in pCO_2 treatments above 1500 µatm than the 400 µatm control (Figure 5D). However, while pCO_2 did have a significant effect on the inorganic content of repaired shell ($p=0.013$, Table S2, Figure 5E), no effect was observed on the force required to dislodge repair patches ($p=0.263$, Table S2, Figure 5F). No effect of OA was also observed on the mean ($p=0.85$, Figure 6C) or max ($p=0.56$, Figure 6D) grayscale values approximating the shell density of repaired region collected from µCT scans (Table S4).

The condition ($p<0.001$) and gonad ($p=0.008$) indices of mussels universally decreased over 10 weeks under laboratory conditions (Table S5, Figure S2A,D). Mussel condition ($p=0.017$), not reproductive condition ($p=0.814$), was significantly affected by pCO_2 and no interaction with time in treatment was detected ($p=0.645$, Table S3). When comparing the initial and final condition and gonad indices under experimental conditions, a significant impact of pCO_2 on CI ($p<0.001$) and GI ($p=0.012$) was observed, with no decrease in either metric observed in field populations over the same time period (Table S5, Figure S1). However, neither CI or GI was correlated with the force to dislodge repaired regions ($p=0.435$, $p=0.690$) or their inorganic content ($p=0.989$, $p=0.619$), with no observed clustering observed with pCO_2 treatment (Figure S2).

4. Discussion

Here we describe the shell repair process of mytilid mussels after sublethal shell damage that penetrates the mantle cavity away from the shell margin, as well as the effect of ocean acidification (OA) on the speed and efficiency of repair. In both field and laboratory assays, mussels mineralized shell injuries within 3 weeks, transitioning through four distinct repair stages wherein the inorganic content, structural integrity, and shell density of repaired shell increased (Figure 2, Figure 4). The ability of mussels to close simulated bore holes was not impacted by environmental pCO_2 (Figure 5A), with no effect of OA observed on the strength (Figure 5F) or density (Figure 6) of repaired shell after 10-weeks under laboratory conditions. However, as mussels progressed through each repair stage, significant interactions between pCO_2, the length of exposure to treatment conditions, and the strength, inorganic content, and physiological condition of mussels within OA treatments were observed (Table S3, Figure 5). These results suggest that, while OA (up to 2500 µatm) may not prevent mussels from repairing shell damage, sustained exposure to increased pCO_2 may induce physiological stress responses that impose energetic constraints on aspects of the shell repair process.

Our field observations indicate that up to 8% of mussel populations carry evidence of shell damage consistent with the feeding strategy of predatory gastropods (Figure 1). To limit exposure to the surrounding environment, mussels in both field and laboratory conditions quickly (within 5 days) covered 1 mm diameter drill holes by affixing an organic film over the interior of the shell opening (Figure 2A, Figure 3A-C). The texture and color of organic film was consistent with the findings of prior studies, several of which have characterized the composition of numerous matrix proteins and polysaccharides [68-70]. µCT imaging of repaired shells confirmed that these films formed over, rather than within, drill holes, similar to the way a patch is applied over a tear in a piece of clothing (Figure 4, Figure 6A).

Significant variability was observed between individual mussels' initial response to shell injury, irrespective of pCO2 treatment. Organic films typically covered drill holes, but varied widely in their size, shape, and even location with respect to the shell injury (Figure 3A-E); 10% of mussels produced a patch 100x greater than the drill hole diameter (Figure 3F) and, in rare instances, organic matrix was produced away from shell damage altogether (Figure 3E). To our knowledge, variability in the localization of the repair process of this magnitude has not been previously reported. One possible explanation for this variation could be that, while great lengths were taken to standardize the depth with which drill holes were generated, variation in shell thickness may have resulted in different degrees of tissue damage. Additionally, shell fragments from drilling could have been dispersed within the shell cavity, leading to non-localized repair. While there is evidence that specific proteins act as nucleation sites during calcite and aragonite formation [71,72], less is known about how mollusks determine where to deposit the organic matrix. Work by Hüning et al. (2016) [46] provides preliminary evidence that the expression of genes involved in shell formation at the pallial and marginal mantle can be induced in central mantle tissue after shell damage. The results presented here suggest that transcriptomic changes in the mantle that lead to organic matrix deposition may be part of a more globalized physiological response than previously thought, or mediated by some yet unknown factor with regard to the type of shell injury endured.

Irrespective of individual variation in organic film formation, the strength and inorganic content of the repaired region increased as time passed after shell damage (Figure 2, Figure 4). This result is consistent with other studies that monitor shell formation, which have observed that calcium carbonate precipitation into the organic matrix acts as a precursor to aragonite formation [73,74]. Shell mineralization was also apparent visually, as the color of deposited organic matrix transitioned from a greenish-yellow to what appeared to be a mixture of crystalline gray structures during S2 (Figure 2A). While it remains unclear to what extent the rate of progression through

each repair stage is influenced by mussel condition or seasonal factors, other studies using drill-based shell damage assays have observed a similar chronological hierarchy of protein secretion (6-15 d), calcite crystal accumulation (15-23 d), and aragonite tablet formation (30-100 d) after the initial shell injury [28,46]. In our field experiment with *M. edulis*, all mussels after 27 days showed evidence of mineralization at the repair site, with aragonite formation at 51 days (Figure 2C). The same process was seen in the laboratory with *M. trossulus*, where mussels produced organic films as early as 5 days (Figure 2B) and evidence of calcite accumulation was observed after 22 days (Figure 4).

Mussels (*M. trossulus*) repairing damaged shells within seven pCO_2 treatments ranging from 400 to 2500 µatm for 10-weeks do not exhibit evidence of direct OA impacts on the shell repair process. Mussels generally reached S1 level of repair after 22 days regardless of OA treatment (Figure 5A), and there was no evidence that the strength (Figure 5F) or density (Figure 6C,D) of repaired shell was impacted by pCO_2 in individuals collected after exposure to OA for 10-weeks. However, a significant interaction between pCO_2 and the time spent in each OA treatment was observed for both the strength (force to dislodge) and inorganic content of repaired shell (Table S1), as well as a trend of more mussels remaining in S2 after 10-weeks in high pCO_2 treatments (Figure 5D).

Observed associations between OA and the composition or strength of repaired shell in this study is complicated by an overall decline in the physiological and reproductive condition of mussels across all treatments over the course of 10-weeks, along with a significant interaction between condition index and pCO_2. There is substantial evidence that adult mussels can produce shell under physiologically stressful conditions, and many species persist in upwelling zones where CO_2 rich waters can lead to calcium carbonate saturation states well below 1 [75]. Subsequent observations of the total calcium carbonate production of mussel beds within these

regions also suggest that the degree to which OA impacts shell production strongly depends on habitat food density (particulate organic carbon, POC) [76,77], and pales in comparison to the effect of warming [42]. In our laboratory experiment, all mussels were fed 5% of their wet body mass in algae daily, delivered at a concentration of 3,000-10,000 cells ml^{-1} with peristaltic pumps at regular intervals. This amount of food was consistent with previous studies in our laboratory where mussels have maintained and even gained tissue mass over the course of 3 months (Carrington et al., unpublished dataset). However, the condition of mussels within our experiment, as denoted by the ratio of grams of dried tissue to shell length cubed, decreased as both a function of pCO_2 treatment ($p=0.008$) and time ($p=0.001$) with an interaction that was also significant ($p=0.030$, Table S5). As a point of comparison, wild populations of mussels over this same time period did not experience a significant decrease in either physiology condition or gonad index (Table S5, Figure S1), making any observed effects of pCO_2 on shell repair within our mesocosm study difficult to ascribe to OA alone.

To our knowledge, this study is the first to investigate the impact of OA on the structure, composition, and integrity of repaired shell in mytlid mussels away from the shell margin. A number of studies have investigated the impact of shell repair in gastropods [78-80], and previous work in mussels has described transcriptomic shifts in mantle gene expression in response to OA [81,82]. The combination of OA and increased temperature (Li *et al.*, 2015). Hüning et al. (2013) show that exposure to OA up to 4000 µatm for 8-weeks reduced the expression of genes related to energy and protein metabolism, as well as greatly depressed the expression of key proteins that facilitate the calcification process (e.g., chitinase) expression in the inner mantle (central zone), the region likely responsible for shell repair in drill-based assays such as the one described here. However, it is worth noting that sustained exposure to OA conditions below a pH of 7.3 (the most extreme treatment used in this study) is unlikely, even in nearshore environments [8], despite high frequency excursions in pH observed in estuarine habitats [6,7].

Taken together, our results suggest that if OA does have an effect on shell repair in mussels, it is likely through the induction of energetic constraints on biomineralization [83,84]. Biomineralization is an energy intensive process [85,86], and the added cost of shell repair (maintenance) could impose energetic limitations on other physiological processes such as growth or reproduction [87]. In areas where mussels sustain a high rate of shell damage, it is possible that the cost associated with shell repair could compound over time, preventing smaller individuals from quickly surpassing the size range in which larger predators (e.g., sea stars, crustaceans) can handle them [88]. However, there is growing evidence that, given adequate food availability, mussels possess mechanisms to reduce the cost of shell repair, such as shell thickening [89,90] or perpetual shell remodeling [91]. To tease apart these interactions, future work would benefit from integrating biomechanical, material, and genetic techniques to describe the shell repair process in different environmental conditions and under different degrees of food limitation.

5. Funding Information

This work was supported by NSF award #DBI-0829486 to K. Sebens, T. Klinger and J. Murray, and by NSF awards #EF-104113 and OCE-2050273 to E. Carrington.

6. Data Availability

Data are archived under project #2250 at www.bco-dmo.org.

7. Author Contributions

MNG, MJO, and EC conceived of the study. MC and EC conducted mussel bed surveys and performed the shell repair field assay using *M. edulis*. MNG and MJO conducted the ocean acidification experiment with *M. trossulus* and completed mechanical testing, material

composition assays, and µCT analyses. MNG and EC performed data analysis and wrote the manuscript. All authors gave final approval for publication.

8. Conflict of Interest

The authors declare no conflict of interest.

9. Acknowledgements

We are grateful for the logistical and technical support of Rainah Sandstrom, Nicki LeBaron, Hilary Hayford, Laura Newcomb, and Michelle Herko. A special thank you to Timothy Cox at Seattle Children's Research Institute and Ben Marwick of the University of Washington Anthropology Department for sharing their expertise and resources.

10. References

1. Gutiérrez, J.L.; Jones, C.G.; Strayer, D.L.; Iribarne, O.O. Mollusks as ecosystem engineers: the role of shell production in aquatic habitats. *Oikos* **2003**, *101*, 79-90.
2. Vaughn, C.C.; Hoellein, T.J. Bivalve impacts in freshwater and marine ecosystems. *Annual Review of Ecology, Evolution, and Systematics* **2018**, *49*, 183-208.
3. FAO. Fisheries and Aquaculture topics. The State of World Fisheries and Aquaculture (SOFIA). Topics Fact Sheets. Text by Jean- Francois Pulvenis. *FAO Fisheries Division [online]* **2020**.
4. Vermeij, G.J. *A natural history of shells*; Princeton University Press: 1995; Volume 15.
5. Hofmann, G.E.; Smith, J.E.; Johnson, K.S.; Send, U.; Levin, L.A.; Micheli, F.; Paytan, A.; Price, N.N.; Peterson, B.; Takeshita, Y. High-frequency dynamics of ocean pH: a multi-ecosystem comparison. *PloS one* **2011**, *6*, e28983, doi:10.1371/journal.pone.0028983.
6. Frieder, C.; Nam, S.; Martz, T.; Levin, L. High temporal and spatial variability of dissolved oxygen and pH in a nearshore California kelp forest. *Biogeosciences* **2012**, *9*, doi:10.5194/bg-9-3917-2012.
7. George, M.N.; Andino, J.; Huie, J.; Carrington, E. Microscale pH and dissolved oxygen fluctuations within mussel aggregations and their implications for mussel attachment and raft aquaculture. *Journal of Shellfish Research* **2019**, *38*, 795-809, doi:10.2983/035.038.0329.
8. Lowe, A.T.; Bos, J.; Ruesink, J. Ecosystem metabolism drives pH variability and modulates long-term ocean acidification in the Northeast Pacific coastal ocean. *Scientific reports* **2019**, *9*, 1-11, doi:10.1038/s41598-018-37764-4.
9. Bates, N.; Best, M.; Neely, K.; Garley, R.; Dickson, A.; Johnson, R. Detecting anthropogenic carbon dioxide uptake and ocean acidification in the North Atlantic Ocean. *Biogeosciences Discussions* **2012**, *9*, doi:10.5194/bgd-9-989-2012.

10. Doney, S.C.; Fabry, V.J.; Feely, R.A.; Kleypas, J.A. Ocean acidification: the other CO2 problem. **2009**, doi:10.1146/annurev.marine.010908.163834.
11. Gazeau, F.; Parker, L.M.; Comeau, S.; Gattuso, J.-P.; O'Connor, W.A.; Martin, S.; Pörtner, H.-O.; Ross, P.M. Impacts of ocean acidification on marine shelled molluscs. *Marine biology* **2013**, *160*, 2207-2245, doi:10.1007/s00227-013-2219-3.
12. Clements, J.C.; Chopin, T. Ocean acidification and marine aquaculture in North America: potential impacts and mitigation strategies. *Reviews in Aquaculture* **2017**, *9*, 326-341.
13. Halpern, B.S.; Walbridge, S.; Selkoe, K.A.; Kappel, C.V.; Micheli, F.; D'Agrosa, C.; Bruno, J.F.; Casey, K.S.; Ebert, C.; Fox, H.E. A global map of human impact on marine ecosystems. *science* **2008**, *319*, 948-952.
14. Carrington, E.; Moeser, G.M.; Dimond, J.; Mello, J.J.; Boller, M.L. Seasonal disturbance to mussel beds: field test of a mechanistic model predicting wave dislodgment. *Limnology and Oceanography* **2009**, *54*, 978-986.
15. Menge, B.A.; Berlow, E.L.; Blanchette, C.A.; Navarrete, S.A.; Yamada, S.B. The keystone species concept: variation in interaction strength in a rocky intertidal habitat. *Ecological monographs* **1994**, *64*, 249-286.
16. Paine, R.T. Intertidal community structure. *Oecologia* **1974**, *15*, 93-120.
17. Hughes, R.; Dunkin, S.d.B. Behavioural components of prey selection by dogwhelks, Nucella lapillus (L.), feeding on mussels, Mytilus edulis L., in the laboratory. *Journal of Experimental Marine Biology and Ecology* **1984**, *77*, 45-68, doi:10.1016/0022-0981(84)90050-9.
18. Rovero, F.; Hughes, R.N.; Chelazzi, G. Cardiac and behavioural responses of mussels to risk of predation by dogwhelks. *Animal Behaviour* **1999**, *58*, 707-714, doi:10.1006/anbe.1999.1176.
19. Andrews, E. The fine structure and function of the salivary glands of Nucella lapillus (Gastropoda: Muricidae). *Journal of Molluscan Studies* **1991**, *57*, 111-126.
20. Clelland, E.S.; Saleuddin, A. Vacuolar-type ATPase in the accessory boring organ of Nucella lamellosa (Gmelin)(Mollusca: Gastropoda): role in shell penetration. *The Biological Bulletin* **2000**, *198*, 272-283.
21. Hunt, H.L.; Scheibling, R.E. Effects of whelk (Nucella lapillus (L.)) predation on mussel (Mytilus trossulus (Gould), M. edulis (L.)) assemblages in tidepools and on emergent rock on a wave-exposed rocky shore in Nova Scotia, Canada. *Journal of Experimental Marine Biology and Ecology* **1998**, *226*, 87-113, doi:10.1016/S0022-0981(97)00239-6.
22. Menge, B.A. Predation intensity in a rocky intertidal community. *Oecologia* **1978**, *34*, 17-35, doi:10.1007/BF00346238.
23. Carriker, M.R. Excavation of boreholes by the gastropod, Urosalpinx: an analysis by light and scanning electron microscopy. *American Zoologist* **1969**, *9*, 917-993, doi:10.1093/icb/9.3.917.
24. Reyment, R.A. Paleoethology and fossil drilling gastropods. *Transactions of the Kansas Academy of Science (1903)* **1967**, 33-50.
25. Kaehler, S.; McQuaid, C. Lethal and sub-lethal effects of phototrophic endoliths attacking the shell of the intertidal mussel Perna perna. *Marine Biology* **1999**, *135*, 497-503, doi:10.1007/s002270050650.
26. Burnett, L.E. Physiological responses to air exposure: acid-base balance and the role of branchial water stores. *American Zoologist* **1988**, *28*, 125-135, doi:10.1093/icb/28.1.125.
27. Harper, E.M. The molluscan periostracum: an important cnstraint in bivalve evolution. *Palaeontology* **1997**, *40*, 71-91.
28. Uozumi, S.; Suzuki, S. " Organic Membrane-Shell" and Initial Calcification in Shell Regeneration. *北海道大学理学部紀要* **1979**, *19*, 37-74.

29. Kadar, E.; Lobo-da-Cunha, A.; Azevedo, C. Mantle-to-shell CaCO 3 transfer during shell repair at different hydrostatic pressures in the deep-sea vent mussel Bathymodiolus azoricus (Bivalvia: Mytilidae). *Marine biology* **2009**, *156*, 959-967.
30. Marin, F.; Luquet, G. Molluscan biomineralization: The proteinaceous shell constituents of Pinna nobilis L. *Materials Science and Engineering: C* **2005**, *25*, 105-111, doi:10.1016/j.msec.2005.01.003.
31. Palmer, A. Relative cost of producing skeletal organic matrix versus calcification: evidence from marine gastropods. *Marine Biology* **1983**, *75*, 287-292.
32. Palmer, A.R. Calcification in marine molluscs: how costly is it? *Proceedings of the National Academy of Sciences* **1992**, *89*, 1379-1382, doi:10.1073/pnas.89.4.1379.
33. Gazeau, F.; Quiblier, C.; Jansen, J.M.; Gattuso, J.P.; Middelburg, J.J.; Heip, C.H. Impact of elevated CO2 on shellfish calcification. *Geophysical research letters* **2007**, *34*, doi:10.1029/2006GL028554.
34. Waldbusser, G.G.; Hales, B.; Langdon, C.J.; Haley, B.A.; Schrader, P.; Brunner, E.L.; Gray, M.W.; Miller, C.A.; Gimenez, I. Saturation-state sensitivity of marine bivalve larvae to ocean acidification. *Nature Climate Change* **2015**, *5*, 273-280, doi:10.1038/nclimate2479.
35. Pörtner, H.O.; Langenbuch, M.; Reipschläger, A. Biological impact of elevated ocean CO 2 concentrations: lessons from animal physiology and earth history. *Journal of Oceanography* **2004**, *60*, 705-718.
36. Orr, J.C.; Fabry, V.J.; Aumont, O.; Bopp, L.; Doney, S.C.; Feely, R.A.; Gnanadesikan, A.; Gruber, N.; Ishida, A.; Joos, F. Anthropogenic ocean acidification over the twenty-first century and its impact on calcifying organisms. *Nature* **2005**, *437*, 681-686, doi:10.1038/nature0409.
37. Ries, J.B.; Cohen, A.L.; McCorkle, D.C. Marine calcifiers exhibit mixed responses to CO2-induced ocean acidification. *Geology* **2009**, *37*, 1131-1134, doi:10.1130/G30210A.1.
38. Zhao, X.; Han, Y.; Chen, B.; Xia, B.; Qu, K.; Liu, G. CO2-driven ocean acidification weakens mussel shell defense capacity and induces global molecular compensatory responses. *Chemosphere* **2020**, *243*, 125415, doi:10.1016/j.chemosphere.2019.125415.
39. Gazeau, F.; Gattuso, J.-P.; Dawber, C.; Pronker, A.; Peene, F.; Peene, J.; Heip, C.; Middelburg, J. Effect of ocean acidification on the early life stages of the blue mussel Mytilus edulis. *Biogeosciences* **2010**, *7*, 2051, doi:10.5194/bg-7-2051-2010.
40. Kurihara, H. Effects of CO2-driven ocean acidification on the early developmental stages of invertebrates. *Marine Ecology Progress Series* **2008**, *373*, 275-284, doi:10.3354/meps07802.
41. Gazeau, F.; Alliouane, S.; Bock, C.; Bramanti, L.; López Correa, M.; Gentile, M.; Hirse, T.; Pörtner, H.-O.; Ziveri, P. Impact of ocean acidification and warming on the Mediterranean mussel (Mytilus galloprovincialis). *Frontiers in Marine Science* **2014**, *1*, 62, doi:10.3389/fmars.2014.00062.
42. Mackenzie, C.L.; Ormondroyd, G.A.; Curling, S.F.; Ball, R.J.; Whiteley, N.M.; Malham, S.K. Ocean warming, more than acidification, reduces shell strength in a commercial shellfish species during food limitation. *PLoS One* **2014**, *9*, e86764, doi:10.1371/journal.pone.0086764.
43. Vihtakari, M.; Hendriks, I.E.; Holding, J.; Renaud, P.E.; Duarte, C.M.; Havenhand, J.N. Effects of ocean acidification and warming on sperm activity and early life stages of the Mediterranean mussel (Mytilus galloprovincialis). *Water* **2013**, *5*, 1890-1915, doi:10.1016/j.marenvres.2018.10.007.
44. Fitzer, S.C.; Phoenix, V.R.; Cusack, M.; Kamenos, N.A. Ocean acidification impacts mussel control on biomineralisation. *Scientific reports* **2014**, *4*, 6218.

45. Fitzer, S.C.; Vittert, L.; Bowman, A.; Kamenos, N.A.; Phoenix, V.R.; Cusack, M. Ocean acidification and temperature increase impact mussel shell shape and thickness: problematic for protection? *Ecology and evolution* **2015**, *5*, 4875-4884.
46. Hüning, A.K.; Lange, S.M.; Ramesh, K.; Jacob, D.E.; Jackson, D.J.; Panknin, U.; Gutowska, M.A.; Philipp, E.E.; Rosenstiel, P.; Lucassen, M. A shell regeneration assay to identify biomineralization candidate genes in mytilid mussels. *Marine Genomics* **2016**, *27*, 57-67, doi:10.1016/j.margen.2016.03.011.
47. Waldbusser, G.G.; Hales, B.; Haley, B.A. Calcium carbonate saturation state: on myths and this or that stories. *ICES Journal of Marine Science* **2016**, *73*, 563-568.
48. Carrington, E. Seasonal variation in the attachment strength of blue mussels: causes and consequences. *Limnology and Oceanography* **2002**, *47*, 1723-1733, doi:10.4319/lo.2002.47.6.1723.
49. Carrington, E. The ecomechanics of mussel attachment: from molecules to ecosystems. *Integrative and comparative biology* **2002**, *42*, 846-852, doi:10.1093/icb/42.4.846.
50. Hilbish, T.J.; Bayne, B.L.; Day, A. Genetics of physiological differentiation within the marine mussel genus Mytilus. *Evolution* **1994**, *48*, 267-286, doi:10.1111/j.1558-5646.1994.tb01311.x.
51. Varvio, S.-L.; Koehn, R.K.; Väinölä, R. Evolutionary genetics of the Mytilus edulis complex in the North Atlantic region. *Marine Biology* **1988**, *98*, 51-60, doi:10.1007/BF00392658.
52. Saavedra, C.; Stewart, D.T.; Stanwood, R.R.; Zouros, E. Species-specific segregation of gender-associated mitochondrial DNA types in an area where two mussel species (Mytilus edulis and M. trossulus) hybridize. *Genetics* **1996**, *143*, 1359-1367.
53. Comesaña, A.; Toro, J.; Innes, D.; Thompson, R. A molecular approach to the ecology of a mussel (Mytilus edulis–M. trossulus) hybrid zone on the east coast of Newfoundland, Canada. *Marine Biology* **1999**, *133*, 213-221.
54. Toro, J.; Innes, D.; Thompson, R. Genetic variation among life-history stages of mussels in a Mytilus edulis–M. trossulus hybrid zone. *Marine Biology* **2004**, *145*, 713-725, doi:10.1007/s00227-004-1363-1.
55. Penney, R.W.; Hart, M.J.; Templeman, N.D. Shell strength and appearance in cultured blue mussels Mytilus edulis, M. trossulus, and M. edulis× M. trossulus hybrids. *North American Journal of Aquaculture* **2007**, *69*, 281-295.
56. Carboni, S.; Evans, S.; Tanner, K.E.; Davie, A.; Bekaert, M.; Fitzer, S.C. Are Shell Strength Phenotypic Traits in Mussels Associated with Species Alone? *Aquaculture Journal* **2021**, *1*, 3-13.
57. Baird, R. Measurement of condition in mussels and oysters. *ICES Journal of Marine Science* **1958**, *23*, 249-257, doi:10.1093/icesjms/23.2.249.
58. Rueden, C.T.; Schindelin, J.; Hiner, M.C.; DeZonia, B.E.; Walter, A.E.; Arena, E.T.; Eliceiri, K.W. ImageJ2: ImageJ for the next generation of scientific image data. *BMC bioinformatics* **2017**, *18*, 529.
59. Bell, E.; Gosline, J. Mechanical design of mussel byssus: material yield enhances attachment strength. *Journal of Experimental Biology* **1996**, *199*, 1005-1017.
60. Palmerini, P.; Bianchi, C. Biomass measurements and weight-to-weight conversion factors: a comparison of methods applied to the mussel Mytilus galloprovincialis. *Marine Biology* **1994**, *120*, 273-277, doi:10.1007/BF00349688.
61. O'Donnell, M.J.; George, M.N.; Carrington, E. Mussel byssus attachment weakened by ocean acidification. *Nature Climate Change* **2013**, *3*, 587-590, doi:10.1038/nclimate1846.
62. Martz, T.R.; Connery, J.G.; Johnson, K.S. Testing the Honeywell Durafet® for seawater pH applications. *Limnology and Oceanography: Methods* **2010**, *8*, 172-184.

63. Robbins, L.; Hansen, M.; Kleypas, J.; Meylan, S. CO2calc—a user-friendly seawater carbon calculator for Windows, Max OS X, and iOS (iPhone). *US geological survey open-file report* **2010**, *1280*, 2010.
64. Orr, J.C.; Epitalon, J.-M.; Dickson, A.G.; Gattuso, J.-P. Routine uncertainty propagation for the marine carbon dioxide system. *Marine Chemistry* **2018**, *207*, 84-107.
65. Hu, Y.; Limaye, A.; Lu, J. A new tool for 3D segmentation of computed tomography data: Drishti Paint and its applications. *bioRxiv* **2020**.
66. Fernandez, E. *Johnson: Johnson Transformation. R package version 1.4.*, 2014.
67. FD, M. *Agricolae: statistical procedures for agricultural research.*, 2017.
68. Levi-Kalisman, Y.; Falini, G.; Addadi, L.; Weiner, S. Structure of the nacreous organic matrix of a bivalve mollusk shell examined in the hydrated state using cryo-TEM. *Journal of structural biology* **2001**, *135*, 8-17.
69. Marin, F.; Luquet, G.; Marie, B.; Medakovic, D. Molluscan shell proteins: primary structure, origin, and evolution. *Current topics in developmental biology* **2007**, *80*, 209-276.
70. Weiner, S.; Traub, W. X-ray diffraction study of the insoluble organic matrix of mollusk shells. *FEBS letters* **1980**, *111*, 311-316.
71. Ehrlich, H. Chitin and collagen as universal and alternative templates in biomineralization. *International Geology Review* **2010**, *52*, 661-699.
72. Falini, G.; Albeck, S.; Weiner, S.; Addadi, L. Control of aragonite or calcite polymorphism by mollusk shell macromolecules. *Science* **1996**, *271*, 67-69.
73. Meenakshi, V.; Blackwelder, P.L.; Wilbur, K.M. An ultrastructural study of shell regeneration in Mytilus edulis (Mollusca: Bivalvia). *Journal of Zoology* **1973**, *171*, 475-484.
74. Weiss, I.M.; Tuross, N.; Addadi, L.; Weiner, S. Mollusc larval shell formation: amorphous calcium carbonate is a precursor phase for aragonite. *Journal of Experimental Zoology* **2002**, *293*, 478-491.
75. Melzner, F.; Thomsen, J.; Koeve, W.; Oschlies, A.; Gutowska, M.A.; Bange, H.W.; Hansen, H.P.; Körtzinger, A. Future ocean acidification will be amplified by hypoxia in coastal habitats. *Marine Biology* **2013**, *160*, 1875-1888, doi:10.1007/s00227-012-1954-1.
76. Melzner, F.; Stange, P.; Trübenbach, K.; Thomsen, J.; Casties, I.; Panknin, U.; Gorb, S.N.; Gutowska, M.A. Food supply and seawater p CO 2 impact calcification and internal shell dissolution in the blue mussel Mytilus edulis. *PloS one* **2011**, *6*, e24223.
77. Thomsen, J.; Casties, I.; Pansch, C.; Körtzinger, A.; Melzner, F. Food availability outweighs ocean acidification effects in juvenile M ytilus edulis: laboratory and field experiments. *Global change biology* **2013**, *19*, 1017-1027, doi:10.1111/gcb.12109.
78. Coleman, D.W.; Byrne, M.; Davis, A.R. Molluscs on acid: gastropod shell repair and strength in acidifying oceans. *Marine Ecology Progress Series* **2014**, *509*, 203-211.
79. Cross, E.L.; Peck, L.S.; Harper, E.M. Ocean acidification does not impact shell growth or repair of the Antarctic brachiopod Liothyrella uva (Broderip, 1833). *Journal of Experimental Marine Biology and Ecology* **2015**, *462*, 29-35.
80. Cross, E.L.; Peck, L.S.; Lamare, M.D.; Harper, E.M. No ocean acidification effects on shell growth and repair in the New Zealand brachiopod Calloria inconspicua (Sowerby, 1846). *ICES Journal of Marine Science* **2016**, *73*, 920-926.
81. Hüning, A.K.; Melzner, F.; Thomsen, J.; Gutowska, M.A.; Krämer, L.; Frickenhaus, S.; Rosenstiel, P.; Pörtner, H.-O.; Philipp, E.E.; Lucassen, M. Impacts of seawater acidification on mantle gene expression patterns of the Baltic Sea blue mussel: implications for shell formation and energy metabolism. *Marine Biology* **2013**, *160*, 1845-1861.

82. Martino, P.A.; Carlon, D.B.; Kingston, S.E. Blue Mussel (Genus Mytilus) Transcriptome Response to Simulated Climate Change in the Gulf of Maine. *Journal of Shellfish Research* **2019**, *38*, 587-602.
83. Frieder, C.A.; Applebaum, S.L.; Pan, T.-C.F.; Hedgecock, D.; Manahan, D.T. Metabolic cost of calcification in bivalve larvae under experimental ocean acidification. *ICES Journal of Marine Science* **2017**, *74*, 941-954.
84. Liu, Z.; Zhang, Y.; Zhou, Z.; Zong, Y.; Zheng, Y.; Liu, C.; Kong, N.; Gao, Q.; Wang, L.; Song, L. Metabolomic and transcriptomic profiling reveals the alteration of energy metabolism in oyster larvae during initial shell formation and under experimental ocean acidification. *Scientific Reports* **2020**, *10*, 1-11.
85. Paine, R.T. ENERGY FLOW IN A NATURAL POPULATION OF THE HERBIVOROUS GASTROPOD TEGULA FUNERRALIS 1. *Limnology and Oceanography* **1971**, *16*, 86-98.
86. Rosenberg, G.D.; Hughes, W.W. A metabolic model for the determination of shell composition in the bivalve mollusc, Mytilus edulis. *Lethaia* **1991**, *24*, 83-96.
87. Roberts, E.A.; Newcomb, L.A.; McCartha, M.M.; Harrington, K.J.; LaFramboise, S.A.; Carrington, E.; Sebens, K.P. Resource allocation to a structural biomaterial: Induced production of byssal threads decreases growth of a marine mussel. *Functional Ecology* **2021**, *35*, 1222-1239.
88. Paine, R.T. Size-limited predation: an observational and experimental approach with the Mytilus-Pisaster interaction. *Ecology* **1976**, *57*, 858-873.
89. Cross, E.L.; Harper, E.M.; Peck, L.S. Thicker shells compensate extensive dissolution in brachiopods under future ocean acidification. *Environmental science & technology* **2019**, *53*, 5016-5026.
90. Langer, G.; Nehrke, G.; Baggini, C.; Rodolfo-Metalpa, R.; Hall-Spencer, J.; Bijma, J. Limpets counteract ocean acidification induced shell corrosion by thickening of aragonitic shell layers. *Biogeosciences* **2014**, *11*, 7363-7368.
91. Peck, V.L.; Oakes, R.L.; Harper, E.M.; Manno, C.; Tarling, G.A. Pteropods counter mechanical damage and dissolution through extensive shell repair. *Nature communications* **2018**, *9*, 1-7.

11. Tables and Figures

Table 1. Measured seawater carbonate parameters during OA treatments and their respective variability (±1 SD). Measurement uncertainties for each parameter were as follows: temperature (T; 0.63%), salinity (S; 0.33%), pH (0.13%), and total alkalinity (A_T; 0.19%).

pCO_2 target	**T (°C)**	**Salinity**	**pH (total)**	**A_T (µmol*kgSW)**
400	15.8 ± 0.1	30.0 ± 0.2	7.95 ± 0.03	2079 ± 7
700	16.1 ± 0.5	29.9 ± 0.3	7.77 ± 0.02	2083 ± 8
1000	15.9 ± 0.2	30.2 ± 0.1	7.64 ± 0.02	2080 ± 10
1600	16.0 ± 0.3	30.4 ± 0.2	7.46 ± 0.02	2086 ± 7
1900	16.0 ± 0.2	30.0 ± 0.1	7.38 ± 0.06	2080 ± 6
2200	16.0 ± 0.4	29.8 ± 0.2	7.31 ± 0.03	2078 ± 5
2500	15.9 ± 0.1	30.4 ± 0.3	7.29 ± 0.03	2090 ± 9

Table 2. Calculated seawater parameters over the course of OA treatments and their respective uncertainties. The total uncertainty (U_{total}) for each calculated parameter is reported as the combination of propagated measured uncertainties as reported in Table 1 and the variability of each parameter over the course of each experiment.

pCO_2 target	**pCO_2 (µatm)**	**CO_3 (µmol*kgSW)**	**HCO_3 (µmol*kgSW)**	**Ω_{Ar}**	**Ω_{Ca}**
400	483 ± 64	110 ± 17	1807 ± 38	1.74 ± 0.26	2.73 ± 0.40
700	769 ± 100	77 ± 13	1892 ± 31	1.21 ± 0.22	1.90 ± 0.32
1000	1062 ± 140	58 ± 10	1939 ± 27	0.91 ± 0.16	1.43 ± 0.25
1600	1652 ± 215	39 ± 7	1986 ± 21	0.62 ± 0.11	0.97 ± 0.18
1900	2009 ± 372	34 ± 7	2000 ± 22	0.53 ± 0.11	0.82 ± 0.18
2200	2365 ± 317	28 ± 5	2013 ± 19	0.44 ± 0.08	0.69 ± 0.13
2500	2458 ± 340	27 ± 7	2016 ± 20	0.43 ± 0.09	0.67 ± 0.14

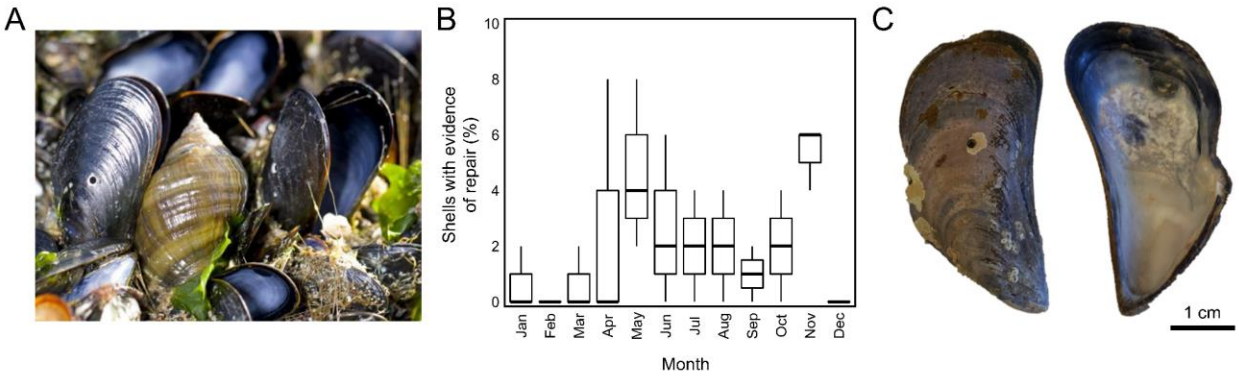

Figure 1. (A) Predation on mussels (*Mytilus edulis*) by predatory gastropods (*Nucella lapillus*; image credit: Luke Miller). (B) Mussels (*M. edulis, n=50 per sample*) with evidence of shell repair over 3 years of monthly field sampling in Rhode Island. (C) Exterior and interior view of a shell (*M. edulis*) with a repaired drill hole collected during field sampling within Rhode Island.

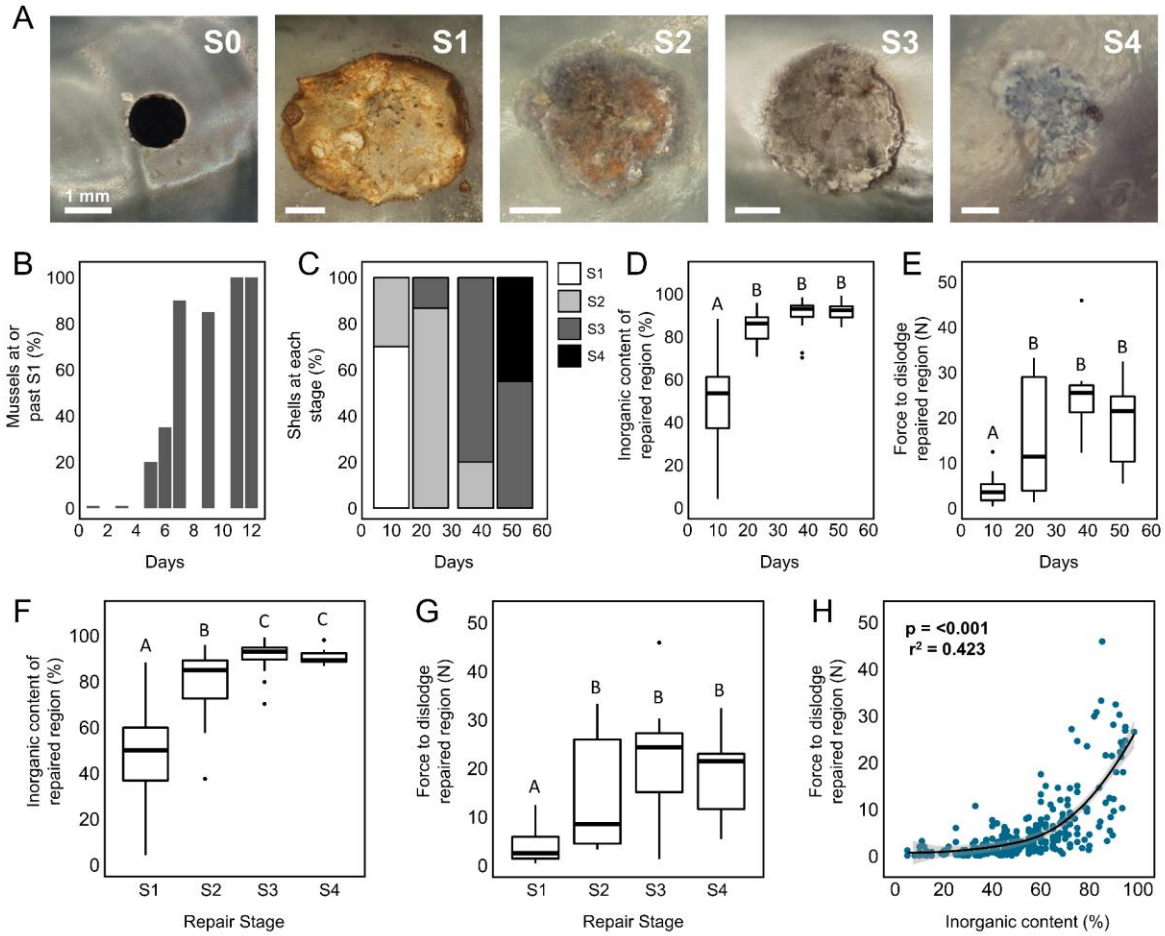

Figure 2. Time series of shell repair process. (A) Photographs of the interior of damaged mussel shells showing the four stereotypical repair stages (S1-S4). (B) Proportion of mussels (*M. trossulus,* n=25) within laboratory experiments that closed drill holes (reached or exceeded S1) over 12 days. Proportion of mussels (*M. edulis,* n=15 per treatment) at each repair stage (C), the inorganic content of excised repaired shell regions (D), and the force required to dislodge repaired shell (E), from out-planted populations sampled over seven weeks in the intertidal. Summary of the inorganic content (F) and force to dislodge (G) repaired shell within each repair stage (pooled data from *M.edulis* and *M. trossulus,* n=282). The relationship between the force and inorganic content of repaired shell (H) across field and laboratory experiments within both mussel species.

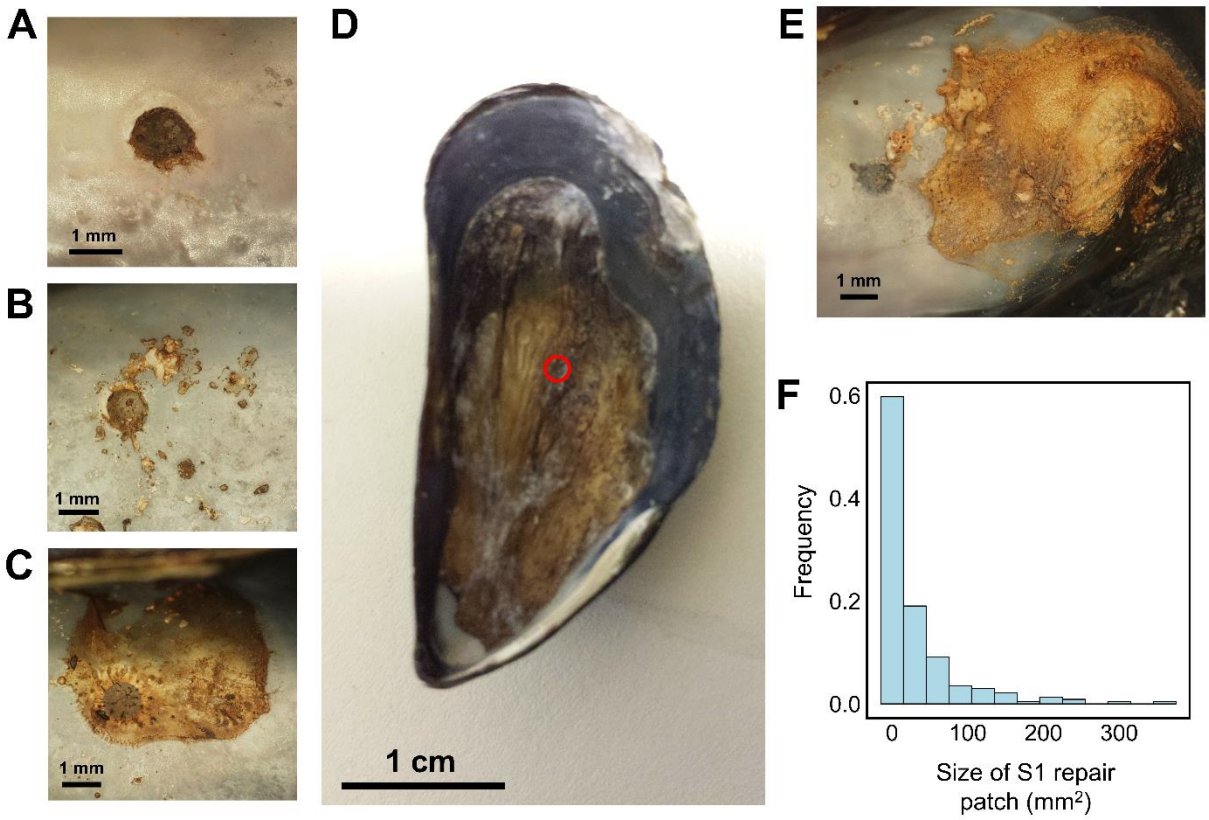

Figure 3. Examples of variable response to shell damage during stage 1 (S1). Some mussels deposited organic matrix neatly within the shell defect (A), while others applied repair patches over a greater area (B-C). In rare cases, the organic matrix encompassed the entirety of the valve interior (D, red circle indicates location of shell damage), while others produced matrix away from the drill hole altogether (E). The frequency distribution of repair patch size during S1 (F).

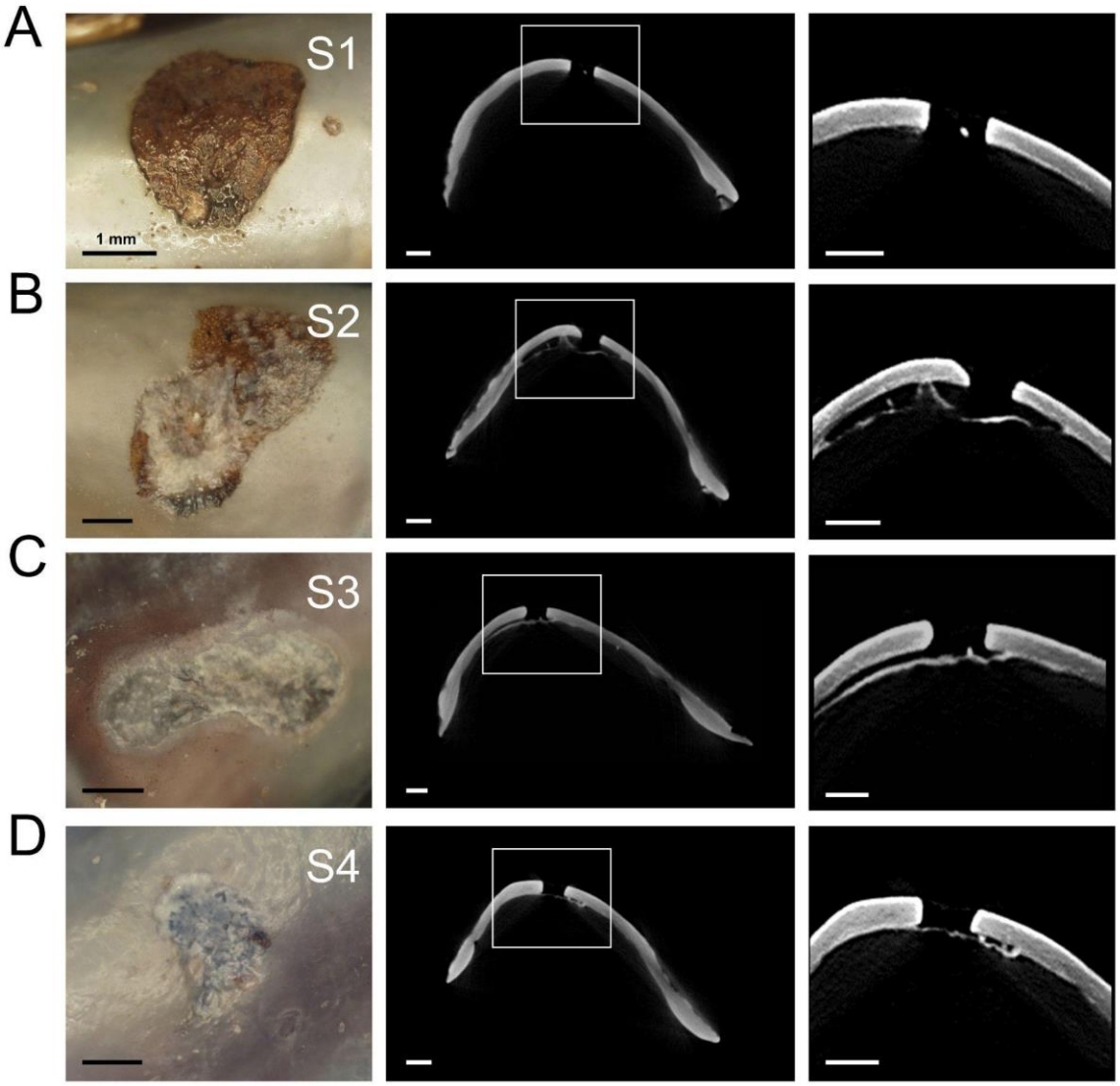

Figure 4. Representative photographs and µCT images of repaired drill holes at each repair stage (S1-4) sampled from mussels within laboratory experiments (*M. trossulus*; 400 µatm pCO_2).

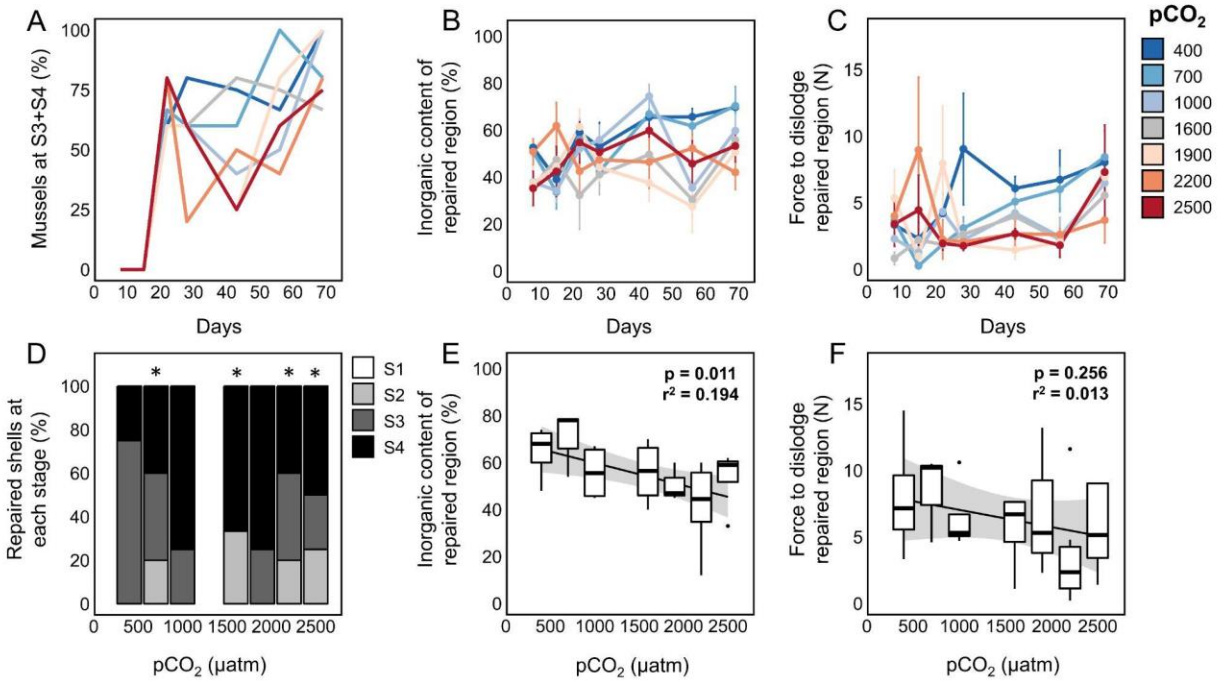

Figure 5. (A) proportion of mussels (*M. trossulus*) that produced mineralized shell (reached S3 or S4) in response to shell damage within each OA treatment. (B) Inorganic content of excised repaired shell from mussels within each OA treatment (C) The force required to dislodge repaired regions produced in each OA treatment. Proportion of mussels at each repair stage (D), the inorganic content of repaired regions (E), and force to dislodge repaired regions (F) after 10 weeks within each OA treatment. Data is from 4-8 mussels per treatment per time point. Asterisks mark treatments that were statistically different than the 400 µatm control.

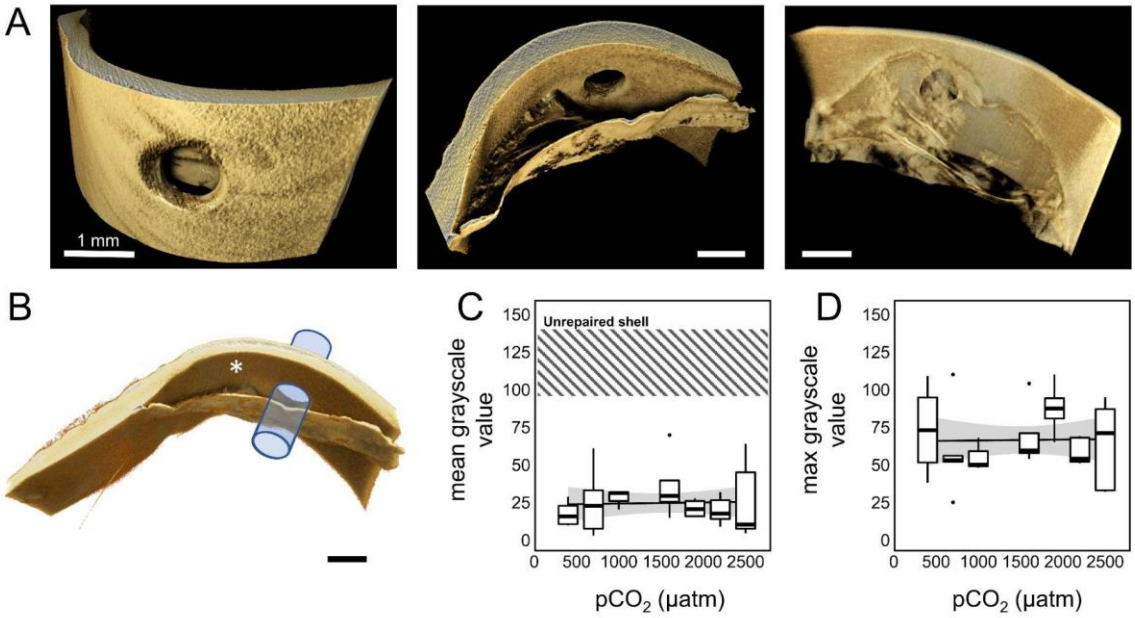

Figure 6. (A) 3D rendering of a drill hole and deposited shell material constructed from µCT scan slices. Images represent three perspectives of the same shell repair from a single mussel (*M. trossulus*) held within the 400 µatm pCO_2 for 10-weeks. (B) Cylindrical volume used for density analysis; asterisk marks approximate location used for control measurements of unrepaired shell. The mean (C) and maximum (D) grayscale values within sampled cylinders after 10-weeks within OA treatments (n=4-8 mussels per treatment).

12. Supplemental Information

Table S1. ANCOVA results comparing the effect of seawater pCO2 and the length of exposure to treatment conditions (days) on the proportion of mussels (M. trossulus) that produced mineralized repaired shell (reached S3 or S4) over 10-weeks.

Source	df	SS	F-value	P-value
Time	6	340.07	48.01	<0.001
pCO_2	6	6.11	0.86	0.53
Residuals	36	42.5		

Table S2. ANOVA results comparing the effect of seawater pCO2 and mussel condition (condition index, CI) on the inorganic content (%) and force required to dislodge repaired shell material (N) within the endpoint population (10-weeks).

Variable	Source	df	SS	F-value	P-value
Inorganic Content	pCO_2	1	1410	7.211	0.013*
	CI	1	10	0.050	0.825
	Residuals	25	4888		
Force	pCO_2	1	25.5	1.313	0.263
	CI	1	5.7	0.291	0.594
	Residuals	25	485.5		

Table S3. ANCOVA results comparing the effect of seawater pCO_2 and the length of exposure (days) to treatment conditions on the force required to dislodge repaired shell (N), the inorganic content of repaired shell (%), the condition index (CI), and gonad index (GI) of mussels over course of 10-weeks within seven OA treatments.

Variable	Source	df	SS	F-value	P-value
Force	Time	6	25.6	5.28	<0.001*
	pCO2	6	12.4	2.57	0.021*
	Time x pCO_2	36	45.7	1.60	0.029*
	Residuals	195	158		
Inorganic content	Time	6	20.8	4.59	<0.001*
	pCO2	6	17.5	3.85	0.001*
	Time x pCO_2	36	53.3	1.96	0.002*
	Residuals	195	147.3		
Repair area	Time	6	0.70	0.72	0.638
	pCO2	6	0.78	0.80	0.573
	Residuals	36	37.7		
CI	Time	6	3.66×10^{-5}	7.55	<0.001*
	pCO2	6	1.28×10^{-5}	2.65	0.017*
	Time x pCO_2	36	2.60×10^{-5}	0.89	0.645
	Residuals	194	1.57×10^{-4}		
GI	Time	6	8.94×10^{-2}	2.98	0.008*
	pCO2	6	1.47×10^{-2}	0.49	0.814
	Time x pCO_2	36	0.047	0.98	0.512
	Residuals	194	0.971		

Table S4. ANCOVA results comparing the effect of seawater pCO_2 on the mean and max grayscale value from µCT scans of endpoint samples (see Figure 6B).

Variable	Source	df	SS	F-value	P-value
Mean grayscale value	pCO_2	6	2.77	0.43	0.85
	Residuals	23	24.5		
Max grayscale value	pCO_2	6	2.77	2.98	0.56
	Residuals	23	2.96×10^2		

Table S5. The results of two-way ANOVA and Tukey HSD comparisons of initial and final (after 10 weeks) condition (condition index, CI) and gonad indices (GI) comparing mussels in OA and field treatments.

	Source	df	SS	F-value	P-value
CI	Treatment	7	26.63	3.72	0.001*
	Time	1	41.53	40.60	<0.001*
	Treatment × Time	7	16.7	2.33	0.030*
	Residuals	110	112.52		
GI	Treatment	7	0.121	2.73	0.012*
	Time	1	0.006	0.95	0.331
	Treatment × Time	7	0.083	1.88	0.080
	Residuals	107	0.674		

	Variable	group		Variable	group
CI	field.initial	a	CI	1600.initial	abc
	field.final	abc		1600.final	abc
	400.initial	abc		1900.initial	a
	400.final	bc		1900.final	bc
	700.initial	ab		2200.initial	ab
	700.final	bc		2200.final	c
	1000.initial	abc		2500.initial	abc
	1000.final	bc		2500.final	abc

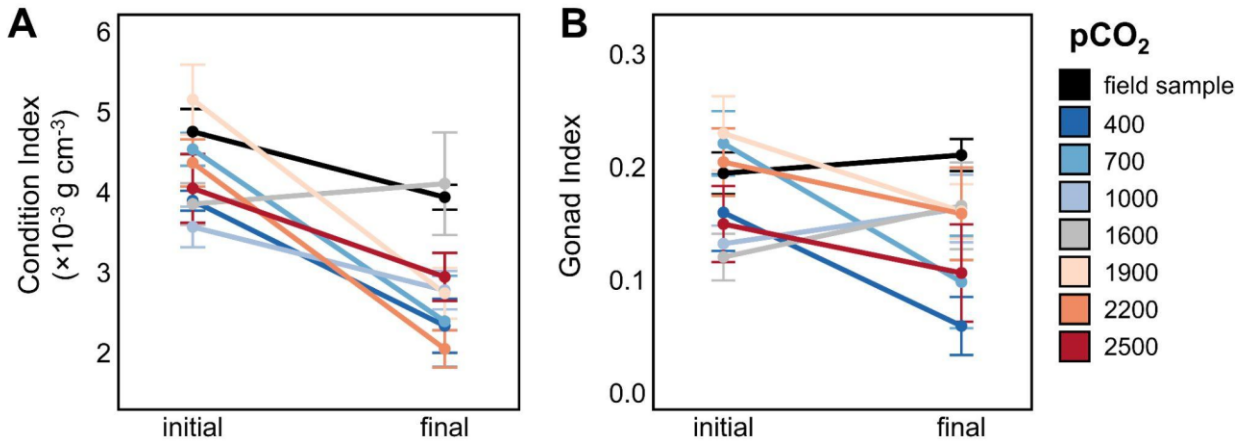

Figure S1. Comparison of the initial and final (after 10 weeks) condition (A) and gonad (B) indices across OA treatments and field samples.

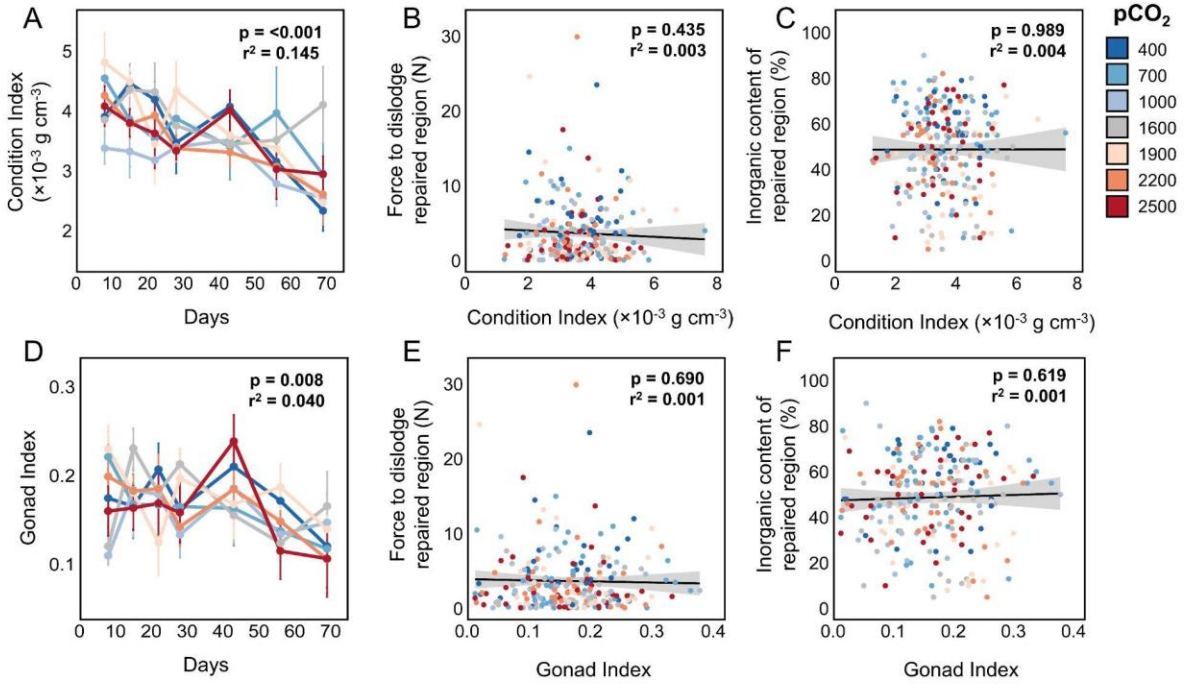

Figure S2. Effect of condition index (CI) and gonad index (CI) on shell repair during OA laboratory experiments. The CI of mussels universally declined under laboratory conditions regardless of OA treatment (A), with no observed effect of CI on the force required to dislodge repaired regions (B) or their inorganic content (C). Similarly, the GI of mussels also declined while housed in the laboratory (D) but did not significantly affect the force to dislodge (E) or inorganic content (F) or repaired shell region.